

Entanglement entropy of two disjoint blocks in critical Ising models

Vincenzo Alba,¹ Luca Tagliacozzo,² and Pasquale Calabrese³

¹*Scuola Normale Superiore and INFN, Pisa, Italy*

²*School of Physical Sciences, The University of Queensland, Queensland 4072, Australia*

³*Dipartimento di Fisica, Università di Pisa and INFN, Pisa, Italy*

(Received 1 February 2010; published 22 February 2010)

We study the scaling of the Rényi and entanglement entropy of two disjoint blocks of critical Ising models as function of their sizes and separations. We present analytic results based on conformal field theory that are quantitatively checked in numerical simulations of both the quantum spin chain and the classical two-dimensional Ising model. Theoretical results match the ones obtained from numerical simulations only after taking properly into account the corrections induced by the finite length of the blocks to their leading scaling behavior.

DOI: [10.1103/PhysRevB.81.060411](https://doi.org/10.1103/PhysRevB.81.060411)

PACS number(s): 75.10.Pq, 64.70.Tg, 03.67.Mn, 05.70.Jk

Conformal field theory (CFT) is one of the most powerful and elegant tools to study quantum one-dimensional (1D) systems and classical two-dimensional (2D) ones. It provides a complete description of the low-energy (large-distance) physics of critical systems that can be classified only on the base of their symmetries.¹ One spectacular recent success was the application of this framework to 2D turbulence.² The predictions of CFT have been tested in experiments for carbon nanotubes,³ spin chains,⁴ and cold atomic gases,⁵ just to cite a few of the most recent ones.

CFT has been traditionally applied to the computation of large distance correlations of local observables. Only recently it has been realized that CFT is also the ideal tool to describe the global properties of a large subset of microscopical constituents (e.g., spins) and in particular their *entanglement*. This has generated an enormous interest in the study of the entanglement properties of many-body systems⁶ that is connecting several branches of physics such as quantum information, condensed matter, and black-hole physics. The quantum information insight about the origin of the achievements of the density-matrix renormalization group (DMRG) in 1D and its failure in higher dimensions⁷ can be cited as an example of the outstanding results generated by this crossover between different branches of physics. The entanglement between two complementary regions A and B of a quantum system described by the state $|\psi\rangle$ can be measured through the entanglement entropy. This is defined as the von Neumann entropy of the reduced density matrix $\rho_A = \text{Tr}_B |\psi\rangle\langle\psi|$ obtained by tracing over the degrees of freedom in the region B. When ψ is the ground state of an infinite 1D critical system and A is a block of length ℓ , CFT predicts the universal scaling⁷⁻⁹

$$S_A = \frac{c}{3} \log \ell + c'_1, \quad (1)$$

where c is the central charge and c'_1 is a nonuniversal constant. This formula is the most effective way to calculate the main signature of the CFT (the central charge), and it can be used to identify the universality class of new models as, for example, done in the Fibonacci chain.¹⁰

The reason of this simple scaling in CFT is easily understood.⁹ In fact, through a replica trick, S_A can be interpreted as $-\partial_n \text{Tr} \rho_A^n|_{n=1}$. For integer n , $\text{Tr} \rho_A^n$ is the partition function on an n -sheeted Riemann surface with two branch points at the border of the interval A that can be mapped to the plane by a conformal transformation. By studying the transformation of the stress-energy tensor under this conformal mapping, one has that $\text{Tr} \rho_A^n$ is the two-point correlation function of some *twist operators* that have scaling dimension $\Delta_n = c/24(n-1/n)$, i.e., $\text{Tr} \rho_A^n = c_n \ell^{-c/6(n-1/n)}$. By analytically continuing this to complex n and by taking the derivative in 1, we get Eq. (1). This reasoning also applies to the case of N intervals: $\text{Tr} \rho_A^n$ is the partition function of a n -sheeted Riemann surface with $2N$ branch points, i.e., a $2N$ -point function of the same twist-operators. A generally incorrect result was obtained by uniformizing this surface.⁹ This is not allowed because of the nonzero genus of the Riemann surface. This result was checked in several free-fermionic theories,¹¹ and only recently, the error has been pointed out.¹²⁻¹⁴ In the case of many intervals, $\text{Tr} \rho_A^n$ turns out to be a function of the full operator content of the theory and not only of the central charge. For a free compactified boson or Luttinger liquid (LL) $\text{Tr} \rho_A^n$ has been calculated for $n=2$ (Ref. 13) and for general integer n .¹⁴ However, the functional dependence on n is so complicated that the analytic continuation has not yet been achieved. These predictions have been checked against the exact diagonalization of the XXZ chain.^{13,14} Unfortunately, the numerical results are limited to relatively small system sizes and only few general properties (such as the dependence on the LL parameter) have been checked: large oscillating corrections to the scaling (as for one block¹⁵) have made impossible a quantitative comparison for the scaling functions related to $\text{Tr} \rho_A^n$. Concepts and calculation schemes used to get these results (such as higher genus Riemann surfaces, twist fields, and orbifold theories) are mathematical tools that have been mainly used in string theory and that only now find their place in condensed-matter physics.

The entanglement of many intervals thus depends on the details of the CFT and should be calculated case by case.¹⁶ The simplest and most studied CFT is the critical Ising model that in the continuum is a free Majorana fermion and

has central charge $c=1/2$. The corresponding 1D quantum spin chain is the Ising model in transverse field described by the Hamiltonian

$$H = - \sum_{j=1}^L [\sigma_j^x \sigma_{j+1}^x + h \sigma_j^z], \quad (2)$$

where $\sigma_j^{x,z}$ are Pauli matrices acting on the spin at site j and we use periodic boundary conditions. The model has a quantum critical point at $h=1$. The correspondence with a free fermion could erroneously lead to the conclusion that S_A for the Ising chain is the incorrect result of Ref. 9, valid for free fermion theories.¹¹ This is not the case when the block A involves more than one interval since the unitary transformation that maps the spin degrees of freedom to the fermionic ones is not anymore contained inside A , as it is easily checked by direct calculation.¹⁷ S_A for two intervals has been calculated in the Ising chain,¹⁸ but for the fermion degrees of freedom and it agrees with Ref. 9. The breaking of the equivalence of fermions and spins makes any lattice exact computation hard, and a representation of ρ_A for two blocks is not yet known. For this reason, we analyze the problem with numerical methods. We use a tree tensor network (TTN) algorithm¹⁹ for the quantum 1D Ising model²⁰ and Monte Carlo simulations of the classical 2D one as in Ref. 12. Using the mapping to the torus partition function for $n=2$, we provide the CFT prediction for $\text{Tr} \rho_A^2$. The generalization of this result to all integer n requires a more detailed analysis (as for the LL,¹⁴ but more difficult because of the complexity of the target space^{21,22}) that we are currently studying and will be reported elsewhere.²³

We consider the case of two disjoint intervals $A = [u_1, u_2] \cup [u_3, u_4]$. By global conformal invariance $\text{Tr} \rho_A^n$ can always be written as^{13,14}

$$\text{Tr} \rho_A^n = c_n^2 \left(\frac{u_{31}u_{42}}{u_{21}u_{32}u_{43}u_{41}} \right)^{(c/6)(n-1/n)} F_n(x), \quad (3)$$

where $u_{ij} = u_i - u_j$ and $x = u_{21}u_{43} / (u_{31}u_{42})$ is the four-point ratio. $F_n(x)$ is the universal scaling function that depends on the theory, and c_n is the nonuniversal factor of the single block. The normalization is $F_n(0) = 1$. The incorrect result of Ref. 9 is $F_n(x) = 1$ identically. For a chain of finite length L , one replaces u_{ij} by the chord distance $L / \pi \sin(\pi u_{ij} / L)$. $F_n(x)$ is symmetric for $x \rightarrow 1-x$.¹³

The TTN (as the better known DMRG) gives the full spectrum of the reduced density matrix. From this S_A and the moments of ρ_A can be extracted and analyzed. The scaling functions $F_n(x)$ [for the entropy $F_{VN}(x) = -F'_1(x)$] are obtained as ratios (difference) of $\text{Tr} \rho_A^n(S_A)$ with the prefactor in Eq. (3). We consider two blocks of length ℓ at distance r . The four-point ratio x is obtained by substituting in its definition the chord distance:

$$x = \left(\frac{\sin \pi \ell / L}{\sin \pi (\ell + r) / L} \right)^2. \quad (4)$$

In the x variable, we would expect that data with different ℓ , r , and L would collapse onto a single curve thus revealing the scaling functions $F_n(x)$.

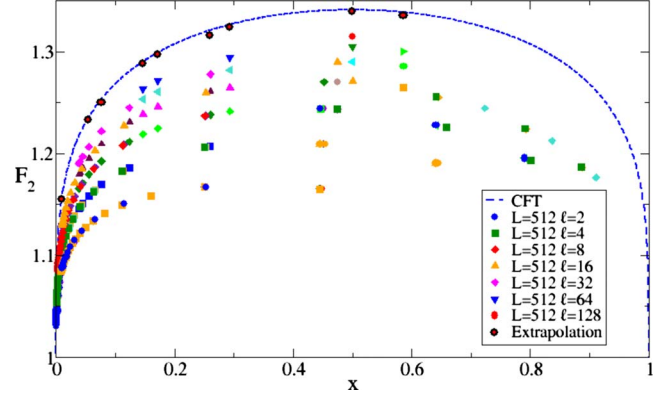


FIG. 1. (Color online) TTN scaling function $F_2(x)$ vs the conformal ratio x for different block sizes ℓ . The upper points are the extrapolation to $\ell \rightarrow \infty$ from Eq. (5). Data for $L \neq 512$ are not shown in the legend. The full line is the CFT prediction [Eq. (6)].

We start our analysis from the data for the function $F_2(x)$ reported in Fig. 1 for ℓ between 2 and 128 and L from 64 to 512. The finite ℓ results do not display the symmetry $x \rightarrow 1-x$, and the data present large corrections to their leading scaling behavior. To extract the asymptotic behavior we perform a finite-size analysis. For any x , general RG arguments give the scaling

$$F_2^{\text{lat}}(x, \ell) = F_2^{\text{CFT}}(x) + \ell^{-\delta_c} f_2(x) + \dots, \quad (5)$$

where δ_c is an unknown exponent, $f_2(x)$ is the scaling function of the first subleading correction, and the dots indicate further ones. The data are well described by $\delta_c = 1/2$. The evidence of this scaling for different x is shown in Fig. 2. It is easy to extrapolate to $\ell \rightarrow \infty$ (the points where the straight lines cross the vertical axis) and the results are reported in Fig. 1. The extrapolation restores the symmetry $x \rightarrow 1-x$. It is possible to calculate this quantity from CFT. In fact, the two-sheeted Riemann surface has the topology of the torus,

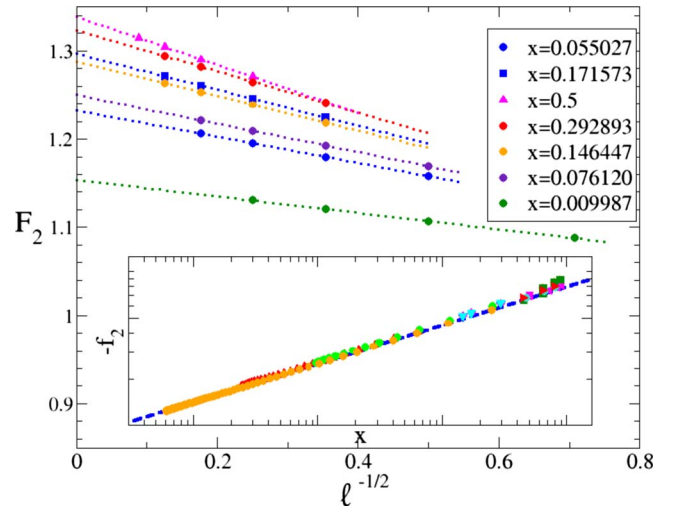


FIG. 2. (Color online) Corrections to the scaling for $F_2^{\text{lat}}(x)$ at fixed x in Eq. (5). Inset: universality of $f_2(x)$. The dashed line is $\propto x^{1/4}$.

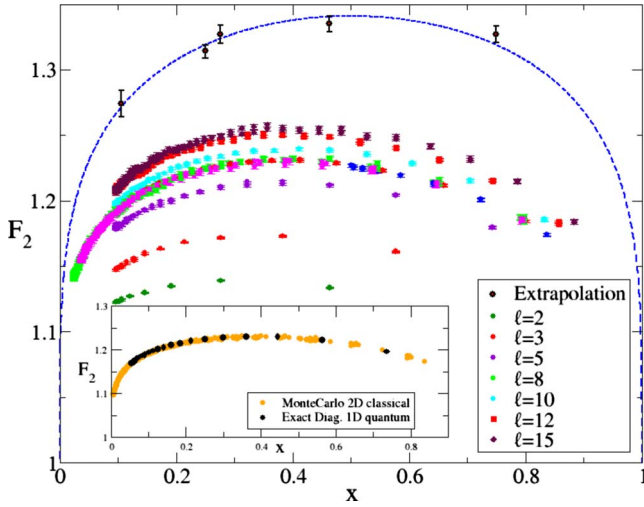


FIG. 3. (Color online) Monte Carlo determination of the scaling function $F_2(x)$. The full line is the CFT prediction [Eq. (6)]. Inset: comparison between Monte Carlo data for the 2D classical Ising model and the exact diagonalization of the quantum chain.

on which it can be mapped by a conformal transformation. The torus partition function for the Ising model is $2Z_{\text{torus}}^2 = (\sum_{\nu=2}^4 |\theta_\nu(\tau)/\eta(\tau)|)^2$,¹ where $\eta(\tau)$ is the Dedekind function, $\theta_\nu(\tau)$ are the Jacobi elliptic functions, and τ is the modular parameter. In our case, τ is given by the solution of $x = [\theta_2(\tau)/\theta_3(\tau)]^4$.²¹ For this value of τ , major simplifications occur [as for $\eta=1/2$ in the LL (Ref. 13)] and the final result can be written in terms of only algebraic functions:

$$F_2(x) = \frac{1}{\sqrt{2}} \left\{ \left[\frac{(1+\sqrt{x})(1+\sqrt{1-x})}{2} \right]^{1/2} + x^{1/4} + [(1-x)x]^{1/4} + (1-x)^{1/4} \right\}^{1/2}. \quad (6)$$

This curve is reported in Fig. 1 and agrees with incredible precision with the extrapolated data. For $x \ll 1$ we have $F_2(x) = 1 + x^{1/4}/2 + \dots$. In the inset of Fig. 2, we report the universal correction to the scaling function $f_2(x)$ obtained as $[F_2^{\text{lat}}(x, \ell) - F_2^{\text{CFT}}(x)]\ell^{1/2}$ for different ℓ that collapse (without any adjustable parameter) on a single curve. In the inset we show $f_2(x) \sim x^{1/4}$.

To check the universality, we study the classical critical 2D Ising model, using the algorithm of Caraglio-Gliozzi to obtain the two-point function of twist-fields.¹² We use an asymmetrical geometry with the temporal direction L_T equal to ten times the spatial one L (between 24 and 324). The results for $F_2(x)$ are reported in Fig. 3 showing the same qualitative features as Fig. 1. The extrapolations to $\ell \rightarrow \infty$ present large error bars but in agreement with CFT. This also implies that a rescaling of all (large enough) length scales should give the same numbers in the two models [as in 2D (Ref. 24)]. The rescaling factor a can be calculated from the single block entanglement obtaining $L_{2D} = aL_{1D}$, with $a \approx 0.71$. In the inset of Fig. 3, the Monte Carlo data for the $L=8$ classical systems are compared with the $L=6$ ($\sim 8 \times 0.71$) quantum chain showing a good agreement.

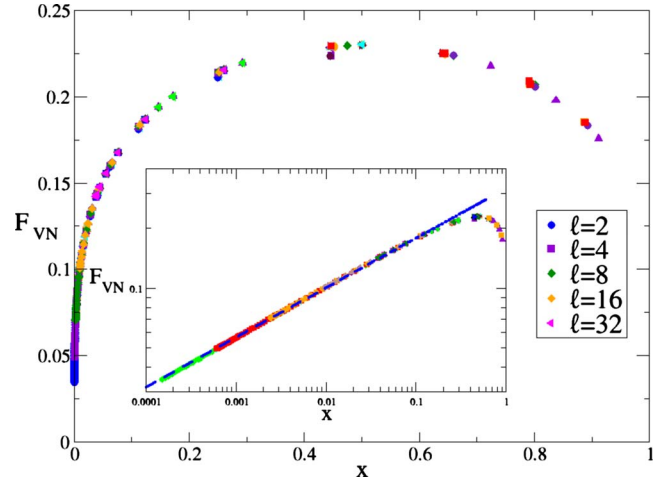


FIG. 4. (Color online) TTN data for the scaling function $F_{VN}(x)$. Corrections to the scaling are negligible and all data collapse. Inset: same data in log-log scale showing the power-law behavior for small x with the predicted exponent $1/4$ and the prefactor π .

In Fig. 4 we report the TTN scaling function for $F_{VN}(x)$. Unfortunately the CFT value is unknown because we are not yet able to make the analytic continuation (as for the LL). One important feature is evident from the plot: the corrections to the scaling are negligible and all data collapse in a single symmetric scaling curve. In the inset of the figure we report the data in log-log scale to emphasize the power-law behavior for small x . In the LL, $F_n(x)$ for small x displays a power law with an n -independent exponent.¹⁴ This reasoning generalizes to the Ising model²³ and from the result for $F_2(x)$ we read that the exponent is $1/4$, as confirmed by the plot. We also found that the prefactor is π . Moreover, for various n , we computed the function $F_n(x)$ for the n th moment of ρ_A also showing large finite ℓ corrections. The analysis of these data will be reported elsewhere.²³

Finally, we consider the full spectrum of ρ_A . If the moments of ρ_A behave like $\text{Tr} \rho_A^n \approx L_{\text{eff}}^{-c(6(n-1/n))}$ with a prefactor

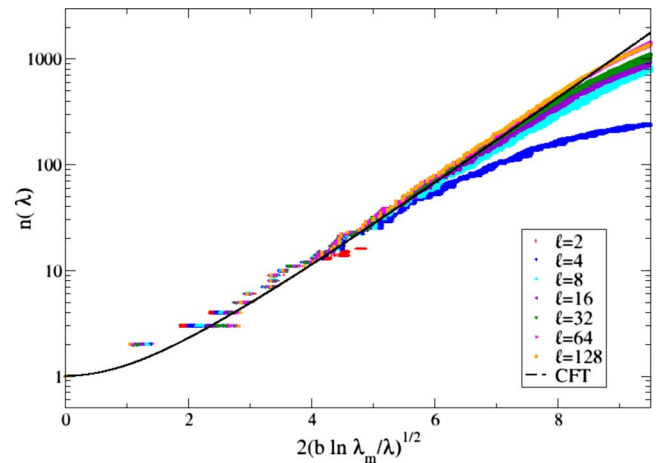


FIG. 5. (Color online) TTN spectrum of the reduced density matrix. In the scaling variable of the horizontal axis all data collapse on the CFT prediction [Eq. (7)].

roughly independent on n , then the spectrum displays the super-universal (i.e., independent on any details of the theory) form²⁵

$$n(\lambda) = \int_{\lambda}^{\lambda_m} d\lambda P(\lambda) = I_0[2\sqrt{b \ln(\lambda_m/\lambda)}], \quad (7)$$

where $n(\lambda)$ is the mean number of eigenvalues larger than λ , λ_m is the maximum eigenvalue, $b = -\ln \lambda_m$, and $I_0(y)$ a Bessel function. This implies that if $n(\lambda)$ is plotted against $y = 2\sqrt{b \ln(\lambda_m/\lambda)}$ all data of any system should collapse on the same curve. In Fig. 5 we plot $n(\lambda)$ against y and all TTN data at different L, ℓ, r (for a total of more than 10^5 points) collapse on the curve predicted by CFT. Finite-size effects are present for small ℓ . Such good agreement is due to the fact that $c_n^2 F_n(x)$ slightly depends on n , varying by few per

cents in the range $[2, \infty]$. This spectrum is fundamental to describe the scaling of numerical algorithms.²⁶

To summarize, we reported a full analytic and numerical analysis of the entanglement of two disjoint intervals in the Ising universality class. This represents the numerical check of the CFT predictions (also derived in this Rapid Communication) for quantities that are more complicated than the entanglement of the single block. It would be interesting to understand how these results change in systems with boundaries (that already for the single interval present intriguing features^{9,27}) and in the presence of quenched disorder, to understand if the apparent “restoration” of conformal invariance for one interval²⁸ is somehow preserved in the case of many.

We are grateful to M. Fagotti, F. Gliozzi, E. Tonni, and G. Vidal for discussions.

¹P. Di Francesco, P. Mathieu, and D. Senechal, *Conformal Field Theory* (Springer-Verlag, New York, 1997).

²D. Bernard *et al.*, Nat. Phys. **2**, 124 (2006); J. Cardy, *ibid.* **2**, 67 (2006).

³H. Ishii *et al.*, Nature (London) **426**, 540 (2003).

⁴M. Klanjšek *et al.*, Phys. Rev. Lett. **101**, 137207 (2008); B. Thielemann *et al.*, *ibid.* **102**, 107204 (2009).

⁵B. Paredes *et al.*, Nature (London) **429**, 277 (2004); T. Kinoshita, T. Wenger, and D. S. Weiss, Science **305**, 1125 (2004); A. H. van Amerongen, J. J. P. van Es, P. Wicke, K. V. Kheruntsyan, and N. J. van Druten, Phys. Rev. Lett. **100**, 090402 (2008).

⁶L. Amico *et al.*, Rev. Mod. Phys. **80**, 517 (2008); J. Eisert, M. Cramer, and M. B. Plenio, *ibid.* **82**, 277 (2010); P. Calabrese, J. Cardy, and B. Doyon, J. Phys. A **42**, 500301 (2009).

⁷G. Vidal, J. I. Latorre, E. Rico, and A. Kitaev, Phys. Rev. Lett. **90**, 227902 (2003); J. I. Latorre *et al.*, Quantum Inf. Comput. **4**, 048 (2004).

⁸C. Holzhey, F. Larsen, and F. Wilczek, Nucl. Phys. B **424**, 443 (1994).

⁹P. Calabrese and J. Cardy, J. Stat. Mech.: Theory Exp. (2004) P06002; Int. J. Quantum Inf. **4**, 429 (2006); J. Phys. A **42**, 504005 (2009).

¹⁰A. Feiguin, S. Trebst, A. W. W. Ludwig, M. Troyer, A. Kitaev, Z. Wang, and M. H. Freedman, Phys. Rev. Lett. **98**, 160409 (2007).

¹¹H. Casini *et al.*, J. Stat. Mech.: Theory Exp. (2005) P05007; J. High Energy Phys. **0903**, 048 (2009); Class. Quantum Grav. **26**, 185005 (2009); I. Klich and L. Levitov, Phys. Rev. Lett. **102**, 100502 (2009).

¹²M. Caraglio and F. Gliozzi, J. High Energy Phys. **0811**, 076 (2008).

¹³S. Furukawa, V. Pasquier, and J. Shiraishi, Phys. Rev. Lett. **102**, 170602 (2009).

¹⁴P. Calabrese, J. Cardy, and E. Tonni, J. Stat. Mech.: Theory Exp. (2009) P11001.

¹⁵P. Calabrese *et al.*, arXiv:0911.4660 (unpublished); B. Nienhuis,

M. Campostrini, and P. Calabrese, J. Stat. Mech.: Theory Exp. (2009) P02063.

¹⁶ S_A measures the entanglement of two intervals with the rest of the system and it is *not* a measure of the entanglement of one interval with respect to the other; see, e.g., H. Wichterich, J. Molina-Vilaplana, and S. Bose, Phys. Rev. A **80**, 010304(R) (2009); S. Marcovitch *et al.*, *ibid.* **80**, 012325 (2009).

¹⁷M. Fagotti (private communication).

¹⁸P. Facchi, G. Florio, C. Invernizzi, and S. Pascazio, Phys. Rev. A **78**, 052302 (2008).

¹⁹M. Fannes, B. Nachtergaele, and R. F. Werner, J. Stat. Phys. **66**, 939 (1992); M. A. Martín-Delgado, J. Rodríguez-Laguna, and G. Sierra, Phys. Rev. B **65**, 155116 (2002); L. Tagliacozzo, G. Evenbly, and G. Vidal, *ibid.* **80**, 235127 (2009).

²⁰The TTN naturally encodes the RG ideas. Tensors are organized in layers corresponding to different length scales (Ref. 19). This makes it particularly suited for finite size studies. Indeed, passing from a smaller system to a bigger one only requires the optimization of a single tensor on the top of the network corresponding to the new length scale.

²¹L. J. Dixon *et al.*, Nucl. Phys. B **282**, 13 (1987).

²²Al. B. Zamolodchikov, Nucl. Phys. B **285**, 481 (1987).

²³V. Alba, P. Calabrese, L. Tagliacozzo, and E. Tonni (unpublished).

²⁴F. Gliozzi and L. Tagliacozzo, J. Stat. Mech.: Theory Exp. (2010) P01002.

²⁵P. Calabrese and A. Lefevre, Phys. Rev. A **78**, 032329 (2008).

²⁶F. Pollmann, S. Mukerjee, A. M. Turner, and J. E. Moore, Phys. Rev. Lett. **102**, 255701 (2009); L. Tagliacozzo, T. R. de Oliveira, S. Iblisdir, and J. I. Latorre, Phys. Rev. B **78**, 024410 (2008); F. Pollmann and J. E. Moore, arXiv:0910.0051 (unpublished).

²⁷N. Laflorencie, E. S. Sørensen, M.-S. Chang, and I. Affleck, Phys. Rev. Lett. **96**, 100603 (2006).

²⁸G. Refael and J. E. Moore, Phys. Rev. Lett. **93**, 260602 (2004); J. Phys. A **42**, 504010 (2009).